Archival Report

Biological Psychiatry

Decoding Depression Severity From Intracranial Neural Activity

Jiayang Xiao, Nicole R. Provenza, Joseph Asfouri, John Myers, Raissa K. Mathura, Brian Metzger, Joshua A. Adkinson, Anusha B. Allawala, Victoria Pirtle, Denise Oswalt, Ben Shofty, Meghan E. Robinson, Sanjay J. Mathew, Wayne K. Goodman, Nader Pouratian, Paul R. Schrater, Ankit B. Patel, Andreas S. Tolias, Kelly R. Bijanki, Xaq Pitkow, and Sameer A. Sheth

ABSTRACT

BACKGROUND: Disorders of mood and cognition are prevalent, disabling, and notoriously difficult to treat. Fueling this challenge in treatment is a significant gap in our understanding of their neurophysiological basis.

METHODS: We recorded high-density neural activity from intracranial electrodes implanted in depression-relevant prefrontal cortical regions in 3 human subjects with severe depression. Neural recordings were labeled with depression severity scores across a wide dynamic range using an adaptive assessment that allowed sampling with a temporal frequency greater than that possible with typical rating scales. We modeled these data using regularized regression techniques with region selection to decode depression severity from the prefrontal recordings.

RESULTS: Across prefrontal regions, we found that reduced depression severity is associated with decreased low-frequency neural activity and increased high-frequency activity. When constraining our model to decode using a single region, spectral changes in the anterior cingulate cortex best predicted depression severity in all 3 subjects. Relaxing this constraint revealed unique, individual-specific sets of spatiospectral features predictive of symptom severity, reflecting the heterogeneous nature of depression.

CONCLUSIONS: The ability to decode depression severity from neural activity increases our fundamental understanding of how depression manifests in the human brain and provides a target neural signature for personalized neuromodulation therapies.

https://doi.org/10.1016/j.biopsych.2023.01.020

Psychiatric and cognitive disorders are among the most challenging ailments in terms of social, economic, and public health toll. This challenge derives in large part from their heterogeneity, in terms of the wide variance in manifestation of these disorders across individuals; and their complexity, in terms of the dearth of objective biomarkers and limited understanding of underlying neurophysiological mechanisms. Adding to their complexity is the fact that networks implicated in psychiatric and cognitive disorders often include prefrontal regions (1,2), which are the most evolutionarily evolved and are particularly challenging to model in nonhuman animals (3). To therapeutically modulate these dysfunctional circuits, a comprehensive understanding of their pathophysiology is needed. The most precise tools available to accomplish this circuit dissection task in humans are electrophysiological recordings and stimulation with intracranial electrodes, given the relatively lower resolution and specificity of noninvasive modalities. Here, we applied this approach to investigate the neurophysiological basis of depression, a common and highly burdensome disorder (4).

Major depressive disorder has a lifetime incidence of 10% to 15% and has immense social and economic consequences (5). It is a major contributor to the overall global burden of disease (6) and in the United States alone accounts for more than $200 billion in health care costs (7). While many conventional treatments are available for depression, nearly one third of patients are resistant to treatment (8). A significant number of depressed patients do not respond to first-line medications even after multiple treatment trials (9). Electroconvulsive therapy and transcranial magnetic stimulation are evidence-based treatments with short-term efficacy, but high rates of relapse are typical (10–12).

Intracranial recordings such as those performed routinely for seizure monitoring (13) provide the requisite degree of spatial, temporal, and spectral specificity for this purpose. Rather than studying the neurophysiological basis of mood regulation in a convenience sample of epilepsy patients undergoing intracranial seizure monitoring (14,15), we did so through a unique clinical trial in a cohort of patients with severe depression and without comorbid epilepsy (4). Advantages of this approach include the fact that the location of recording electrodes can be targeted to depression-relevant regions, instead of being determined purely for seizure monitoring

ISSN: 0006-3223

purposes. Activities during inpatient monitoring can prioritize dense sampling of depression severity measures without concern for interfering with seizure monitoring. The resulting features of interest from the ensuing analyses are more relevant to patients with treatment-resistant depression (TRD) without contamination by processes related to epilepsy.

To achieve our goal of understanding how depression is encoded in the brain, we sought to address two critical questions: 1) What neurophysiological features characterize depressive states? 2) Can we use these features to reliably predict depression severity? The first question entailed finding neural correlates of symptom severity, while the second question addressed the more stringent requirement of finding truly predictive features. As neuromodulatory therapies advance in sophistication, they will be able to incorporate these biomarkers of health and distress. We hope that doing so will allow stimulation therapy to more faithfully (spatially and temporally) match symptomatic demand and thereby improve outcomes.

METHODS AND MATERIALS

Study Design

Subjects with TRD who provided data for this study (N = 3) were enrolled in an early feasibility trial (ClinicalTrials.gov Identifier: NCT03437928) of individualized deep brain stimulation guided by intracranial recordings. The trial is funded by the National Institutes of Health Brain Research Through Advancing Innovative Neurotechnologies (BRAIN) Initiative and approved by the Baylor College of Medicine Institutional Review Board. We conducted this trial under the auspices of an investigational device exemption granted by the U.S. Food and Drug Administration to the principal investigator (SAS). Each subject was implanted with permanent deep brain stimulation leads for stimulation delivery (4) as well as with temporary stereoelectroencephalography (SEEG) electrodes for neural recordings. The analyses here focus on the SEEG recordings, which were obtained across depression-relevant prefrontal regions (Figure 1). Following surgical implant, subjects underwent inpatient monitoring for 9 days, during which we obtained frequent measures of depression severity with simultaneous dense neural recordings.

Depression Severity Measurements

We acquired measurements of depression severity throughout the 9-day inpatient monitoring period using the Computerized Adaptive Test–Depression Inventory (CAT-DI) (16). Each CAT-DI administration typically includes approximately 12 question items selected from a bank of 389 possible items based on real-time feedback from previous items answered by the participant. Using this assessment tool, we collected rapid and relatively frequent measurements of depression severity. The CAT-DI score has been shown to exhibit a strong correlation with other established depression rating scales, such as the 9-item Patient Health Questionnaire and Hamilton Rating Scale for Depression (16). The CAT-DI has high test-retest reliability (r = 0.92), suggesting that score variability is most likely due to symptom variability rather than the natural variance of the test or its adaptive nature (17). A higher CAT-DI score indicates more severe depression symptoms.

Intracranial Recordings and Feature Extraction

We recorded neural signals from the prefrontal SEEG electrode contacts during CAT-DI administration. Herein we refer to each CAT-DI time point and its associated neural data as a block. Signals were recorded at 2 kHz using a Cerebus data acquisition system (BlackRock Microsystems). All signals were amplified and bandpass filtered from 0.3 to 500 Hz (fourth order Butterworth filter). No stimulation was delivered during any of the recordings. We performed notch filtering, bipolar referencing, and Hilbert transform to estimate spectral power features (see the Supplement).

Automatic Region Selection

The recording channels per patient were distributed across 4 main prefrontal regions: anterior cingulate cortex (ACC), dorsolateral prefrontal cortex (PFC), orbitofrontal cortex, and ventromedial PFC. To increase the generalizability of the model and avoid overfitting, we greatly reduced the number of model parameters by using a region selection technique (see the Supplement) (15).

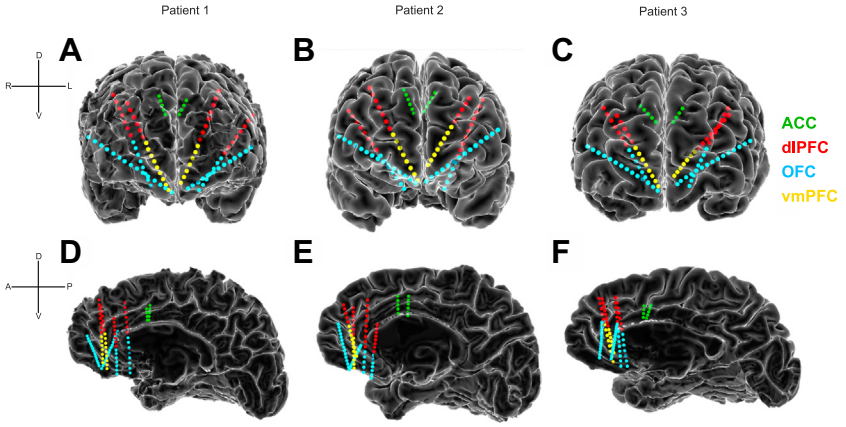

Figure 1. Intracranial recording electrodes sample depression-relevant prefrontal regions. **(A–C)** Frontal views of the reconstructed cortical surface and stereoelectroencephalography recording contacts for patient 1, patient 2, and patient 3, respectively. Stereoelectroencephalography contacts are colored according to the gray matter region sampled: green, anterior cingulate cortex (ACC); red, dorsolateral prefrontal cortex (dlPFC); blue, orbitofrontal cortex (OFC); yellow, ventromedial prefrontal cortex (vmPFC). **(D–F)** Medial views of the reconstructed cortical surface of the right hemisphere (left hemisphere is hidden for visualization purposes). Dorsal (D), ventral (V), left (L), right (R), anterior (A), and posterior (P) directions are indicated.

Model Fitting

We used least absolute shrinkage and selection operator (LASSO) regression to fit neural data to the CAT-DI scores. To assess the performance of our decoder, we performed leave-one-out cross-validation. Permutation test was then used to assess the significance of the predictability (see the Supplement).

RESULTS

Spectral Activity Across Prefrontal Regions Correlates With Depression Severity

Three patients with severe TRD who met eligibility criteria and provided informed consent for the trial were implanted with 2 sets of intracranial electrodes during an initial surgery, one set primarily for stimulating and the other primarily for recording (Figure 1) (4,18). The depression decoding analyses presented here focus on the recording electrodes, which consisted of percutaneously placed temporary SEEG (13) electrodes implanted in brain regions involved in the regulation of mood and cognition: ACC (19–21), dorsolateral PFC (22), orbitofrontal cortex (23,24), and ventromedial PFC (Figure 1) (25). Our clinical trial uses an inpatient intracranial neurophysiology platform to investigate brain-behavior relationships utilizing dense neural recordings and symptom assessments (4). Following the initial implant surgery, patients were monitored in this inpatient monitoring unit for 9 days. We assayed changes in depression severity while simultaneously recording from the implanted electrodes. Clinical outcomes from the first subject in this trial have recently been reported (18).

We measured symptom severity using the CAT-DI, a rapid assessment that correlates with standard depression severity scales (16). The adaptive nature of the CAT-DI allows each administration of this measure to take only 1 to 2 minutes to complete, and its use of a variety of prompts prevents habituation and provides greater confidence with frequent sampling. We observed substantial variation in depression severity in all 3 participants (patient 1: mean [SD] severity score = 78.9 [6.6]; patient 2: mean severity score = 63.0 [4.6]; patient 3: mean severity score = 64.5 [14.1]) over the 9-day monitoring period, with a trend of declining severity over the hospital stay (Figure 2A–C).

To evaluate how neural activity varied throughout the monitoring period, we extracted spectral power from 6 frequency bands: delta (1–4 Hz), theta (4–8 Hz), alpha (8–12 Hz), beta (12–30 Hz), gamma (35–50 Hz), and high-gamma (70–150 Hz), yielding 6 spectral power features per channel for each depression severity measurement. Spectral power features in prefrontal channels showed strong correlations with symptom severity scores after correcting for multiple comparisons. Although there was heterogeneity across patients, power in low frequencies including delta, theta, alpha, and beta were generally positively correlated with symptom severity (92.0% of significant features in patient 1, 99.2% in patient 2, and 88.5% in patient 3 showed a positive correlation with depression severity) (Figure 2D–F), while power in high frequencies including gamma and high-gamma were generally negatively correlated with symptom severity (92.9% of significant features in patient 1, 93.2% in patient 2, and 100.0% in patient 3 showed a negative correlation with depression severity). In all participants, a majority of brain regions demonstrated decreased low-frequency power and increased high-frequency power when symptoms were less severe.

Prefrontal Neural Activity Predicts Depression Severity

The strength of the observed correlations in PFC suggests that depression severity may reliably be predicted from spectral power features. To test this hypothesis, we fit regularized regression models to depression severity scores using neural activity recorded across prefrontal sites. Even with the relatively frequent sampling of depression severity, measurements were sparse (patient 1: 36 measurements; patient 2: 27 measurements; patient 3: 47 measurements) relative to the high dimensionality of neural features (approximately 400 features in each patient). To increase the generalizability of the model, we reduced the dimensionality of the neural data using

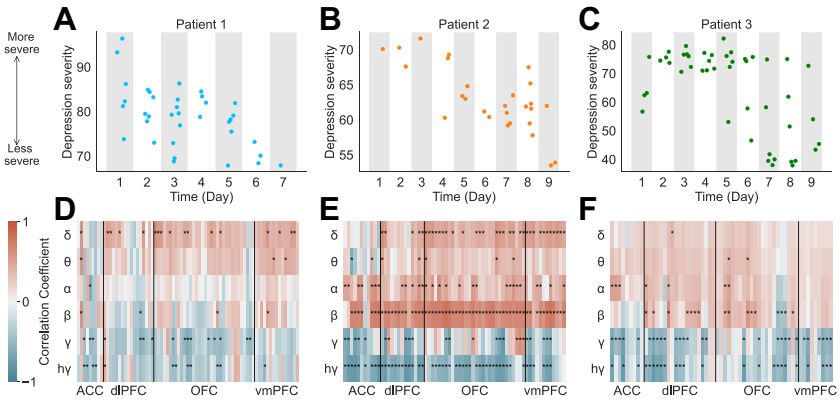

Figure 2. Variation in depression severity captured by neural recordings. **(A–C)** Depression severity (measured by the Computerized Adaptive Test–Depression Inventory tool) varied in all 3 participants. The decreasing trend over time may be related to beneficial effects of stimulation (commonly seen over this timescale), nonspecific therapeutic effects of interactions with the research team, and/or other effects. Regardless of the causes of variation, this approach allowed us to frequently sample depression severity over a wide dynamic range while acquiring concurrent dense prefrontal recordings. **(D–F)** Correlation between severity score and brain activity in all gray matter recordings sites. Each horizontal axis increment is a single recording site; the vertical axis shows the frequency bands. The color indicates the correlation coefficient value between severity score and spectral power. A positive correlation (red) indicates that the severity score increases (more severe depression symptoms) when power increases. A negative correlation (blue) indicates that the severity score decreases (less severe symptoms) when power increases. Features with $p < .05$ after false discovery rate multiple-testing correction are marked with an asterisk. Although there was interindividual variability across specific spatiospectral features, this correlation analysis highlights the trend between low- vs. high-frequency power and depression severity. ACC, anterior cingulate cortex; dlPFC, dorsolateral prefrontal cortex; OFC, orbitofrontal cortex; vmPFC, ventromedial PFC.

automatic region selection and regularized regression. In particular, the model was constrained to use spectral power from a single region to predict depression severity. The selected region was chosen based on the analysis of only training data using a leave-one-out cross-validation strategy. After fitting the model, we used it to predict the depression severity score from a held-out test set and evaluated the prediction error using normalized root mean square error (NRMSE) (15).

Using this approach, we were able to decode depression severity from neural signals in PFC. Our model selected ACC across most folds of cross-validation (all folds in patient 1 and patient 2 and 41 of 47 folds in patient 3), indicating that the ACC was the most informative region for predicting depression severity in all 3 participants (Figure 3A–C). Next, we explored relative feature importance within the ACC. The regression coefficients for each feature indicate feature importance, with larger coefficient magnitudes reflecting greater importance. A few features were consistently more important than others across all folds of the cross-validation and were significantly correlated with symptom severity score (Figure S1). Additionally, there was a strong and significant correlation between predicted and measured symptom score in each participant (patient 1: $r = 0.66$, $p < 10^{-4}$, patient 2: $r = 0.93$, $p < 10^{-4}$, patient 3: $r = 0.68$, $p < 10^{-4}$), indicating high predictive performance (Figure 3D–F). The decoder was also highly predictive when scores were standardized and pooled across all participants ($r = 0.73$, $p < 10^{-4}$) (Figure 3G).

We assessed the significance of the NRMSE with a permutation test to evaluate decoder performance relative to chance. In each patient, we randomly permuted the time indices of severity scores and repeated the same leave-one-out cross-validation process. With the scores permuted and thus mismatched with the neural data, depression severity could no longer be accurately predicted (Figure S2). The prediction accuracies of the decoders were significantly greater than chance performance in all participants (patient 1: NRMSE = 0.75, $p < .01$, patient 2: NRMSE = 0.37, $p < 10^{-4}$, patient 3: NRMSE = 0.72, $p < 10^{-3}$) (Figure 3H–J) and when the scores were pooled across participants (NRMSE = 0.68, $p < 10^{-6}$) (Figure 3K).

Given our observation of decreasing depression severity over time (Figure 2A–C), we tested whether our model was trivially identifying a temporal correlation. To do so, we fit a linear regression model to depression severity over time and computed the residuals (Figure S3A–C). This process effectively decorrelated depression severity with time. We then used the neural data to predict the residuals. The decoders accurately predicted the residuals in all patients ($p < .05$ for all patients, $p < 10^{-6}$ for the scores across patients) (Figure S3D–K), indicating that the neural features, not the progress of time, drove the accurate predictions of depression severity.

To add further confidence to our model, we performed 5-fold cross-validation in addition to our original leave-one-out cross-validation approach. The decoder accurately predicted depression severity in 5-fold cross-validation as well ($p < .01$ for all patients, $p < 10^{-6}$ for the scores across patients) (Figure S4), providing further confidence in the results.

To evaluate the performance of the region selection technique employed for dimensionality reduction, we fit the decoder without automatic region selection. These decoders can still predict depression severity at levels significantly better than chance ($p < .05$ for all patients, $p < 10^{-6}$ for the scores across patients) (Figure S5A–H) but have larger prediction errors than decoders with region selection (Figure S5I–L). Thus, inclusion of region selection improves the decoding accuracy of our model.

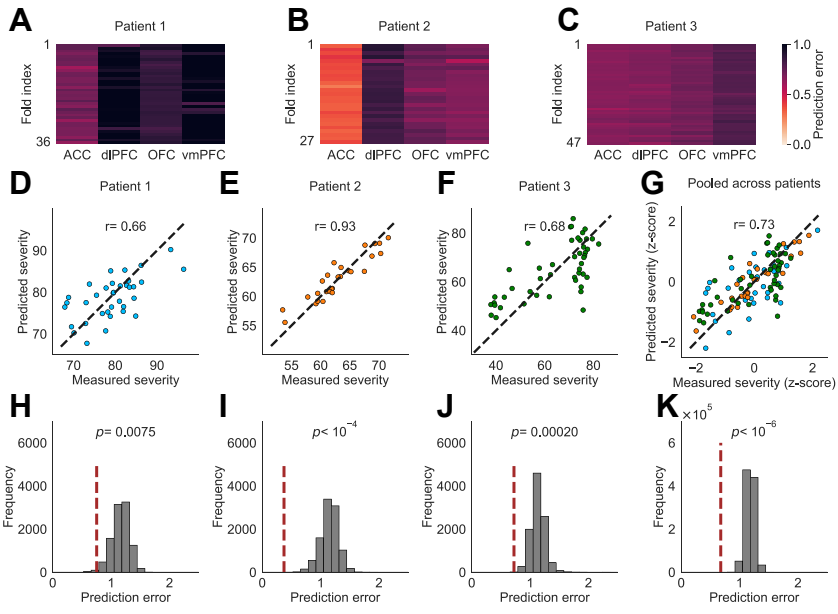

Figure 3. Decoding depression severity from neural activity in prefrontal cortex. **(A–C)** Prediction error of the training set in each fold of the leave-one-out cross-validation. The horizontal axis shows the brain regions, and the vertical axis shows the fold indices of leave-one-out cross-validation. The color indicates the prediction error. Each row includes the prediction error for all regions tested in the training set. Brighter red indicates a smaller error and therefore more accurate prediction. The anterior cingulate cortex (ACC) demonstrated the greatest prediction accuracy across most folds of cross-validation, although its degree of supremacy varied across the 3 subjects. **(D–G)** The predicted score from leave-one-out cross-validation is plotted against the measured score for each depression severity measurement. Points closer to the diagonal indicate more accurate predictions. *r* values denote Pearson correlation coefficients. Scores from patient 1 are shown in blue; scores from patient 2, in orange; and scores from patient 3, in green. **(H–K)** Distribution of the chance level normalized root mean square error computed from leave-one-out cross-validation for sets of permuted scores (gray, 10^4 permuted tests for each patient and 10^6 permuted tests for standardized severity scores pooled across patients). Normalized root mean square error for the model trained with true measured severity scores is shown as a red vertical dashed line. Permutation testing shows that the true prediction error is significantly lower than chance. dlPFC, dorsolateral prefrontal cortex; OFC, orbitofrontal cortex; vmPFC, ventromedial PFC.

Next, we explored the predictability of spectral power from single brain regions and frequency bands (as opposed to all frequency bands) by using these individual features as inputs to the model. While many spectral power features showed significant correlations with depression severity (Figure 2D–F), not all of these features may necessarily be predictive. We trained separate models for each region and frequency band combination and then performed multiple comparison corrections. For patient 1, we found that theta, alpha, and beta power in ACC had significant predictability (Figure 4A). For patients 2 and 3, we observed more widespread predictability across several regions and frequency bands (Figure 4B, C). ACC beta power was the overall most predictive feature in patient 1, whereas ACC high-gamma was most predictive in patients 2 and 3.

To further focus on the neural features that are important for predicting depression severity, we fit the model using all spatial and spectral features without automatic region selection, using a range of values of the regularization parameter alpha to explore the relative importance of individual features. This parameter determines the penalty imposed on the model for including more features. As alpha becomes larger, penalization for adding features increases, and thus fewer features are used. Using ACC beta power, ACC gamma power, and ACC high-gamma power as examples, the fraction of recording channels selected in specific feature groups decreases as the regularization parameter alpha increases (Figure 4D–F). When fitting the model using all individual features, we found that the greatest fraction of channels selected is in ACC, especially when penalization is higher (Figure 4G–I). As penalization decreases and more features are permitted, spectral features in dorsolateral PFC, orbitofrontal cortex, and ventromedial PFC are increasingly included, indicating that informative features for predicting depression severity are not exclusive to the ACC, but instead are distributed across prefrontal cortical regions in various frequency bands and in an individual-specific manner.

It is possible that the neural signals measured during CAT-DI assessments are reflective of cognitive processes engaged by self-evaluation and therefore not specifically related to depression severity per se. To test this alternative hypothesis, we recorded 1-minute resting-state data immediately after each CAT-DI assessment in one subject (patient 3). During this time period, the subject was presumably in a very similar mood state as that during the CAT-DI, but not actively engaged in introspection or any particular cognitive task. We then performed the same analyses on these resting-state recordings as were performed above. Similar to our results using data recorded during the CAT-DI, we observed decreased low-frequency power and increased high-frequency power when symptoms were less severe (Figure S6A). While the model still selected ACC for the plurality of folds for the cross-validation, there was greater distribution across other brain regions (Figure S6B). The predictive power of the model still remained very high (Figure S6C, D). When fitting the model using all individual features, we found a pattern similar to that in the first analysis—that predictive power was greatest in high-frequency features in ACC but distributed across other features as well (Figure S6E–G).

We next assessed the degree of similarity between results derived from the recordings during the CAT-DI assessments versus those from the resting periods. Correlation patterns between spectral power features and depression severity (i.e., Figure 2F and Figure S6A) were very similar ($r = 0.96$, Pearson correlation coefficient, $p < 10^{-4}$), as was predictive power of

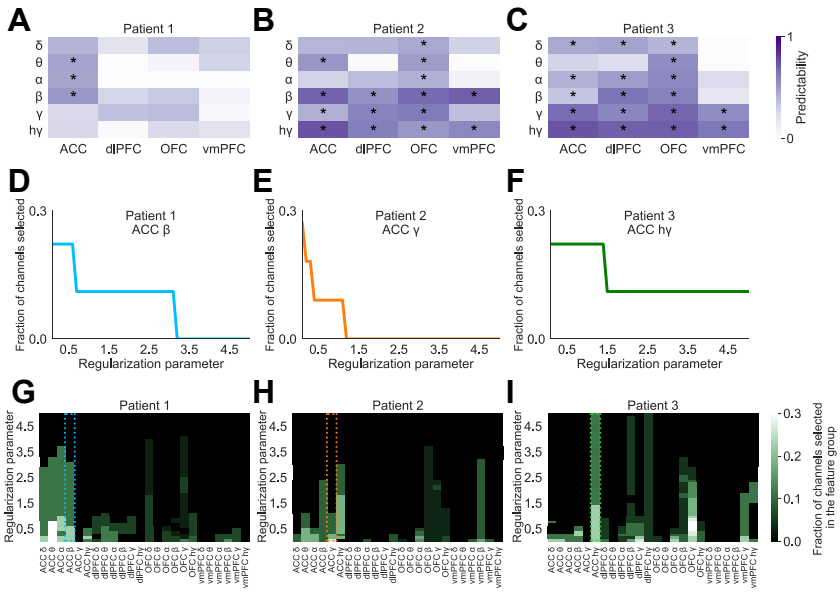

Figure 4. Spatiospectral features for predicting depression severity are specific to the individual. **(A–C)** Predictability of depression severity when using features from a single frequency band in a single brain region. The color indicates the correlation coefficient value between predicted and measured scores. Correlation coefficients with $p <$ .05 (after false discovery rate correction) are marked with an asterisk. Significantly predictive features are restricted to low-frequency bands in anterior cingulate cortex (ACC) in patient 1 but are more distributed across spatiospectral features in patients 2 and 3. **(D–I)** Fraction of recording channels selected in a specific brain region and frequency band as the regularization parameter alpha varies. **(D–F)** As illustrative examples, we show ACC beta power in patient 1, ACC gamma power in patient 2, and ACC high-gamma power in patient 3. At low values of alpha (more permissive of additional features), many features are selected for inclusion in some fraction of recording channels, but a greater fraction is included for features with the most predictive power. As alpha increases, features with the most predictive power survive longer and in a greater fraction of channels. **(G–I)** The same information as in panels **(D–F)** is shown, but as a heatmap and for all features. The 3 examples in panels **(D–F)** are shown with color-corresponding dotted boxes around their respective column. Again, the fraction of recording channels for particular features decreases with increasing alpha. ACC features are selected the most frequently in these patients, but feature distribution is highly individual specific. dlPFC, dorsolateral prefrontal cortex; OFC, orbitofrontal cortex; vmPFC, ventromedial PFC.

spectral features (i.e., Figure 4C and Figure S6E) (r = 0.85, Pearson correlation coefficient, $p < 10^{-4}$). These results further support the conclusion that these neural features are specific to depression severity encoding and also suggest that the differences between analyses performed on recordings during the assessments versus analyses using data from contiguous resting periods are small.

DISCUSSION

Finding neurophysiological features that characterize and even predict symptom severity is critical for improving our understanding of and developing precise treatments for depression. Here, we accurately decoded fluctuations in depression severity over time from intracranially recorded neural activity in 3 patients with TRD. We found that decreased low-frequency power and increased high-frequency power in PFC correlate with lower depression severity (i.e., healthier states). Using these spatiospectral features, we trained a model to predict depression severity and explored the features that were most important for prediction, rather than features that simply showed significant correlations. The transparency and explainability of our model allowed us to identify the ACC as the most influential subregion for decoding depression severity in all 3 patients. Beyond the ACC, we found various individual-specific neurophysiological features distributed across PFC with predictive power. We consider these feature sets to be personalized neural biomarkers for depression severity.

The spectral pattern of correlation we observed—increased high-frequency activity and reduced low-frequency activity—has also been found to be important for decoding positive and negative affect in patients with epilepsy (26). While affective state is not identical to our depression-specific measures, it is likely related. The explainable model we employed was trained on intracranial neural data collected from patients with depression, thus eliminating the confounds of epilepsy comorbidities and possible attendant neurophysiological abnormalities.

The correlation we observed between neural features and improved depression symptoms is reminiscent of similar associations between this spectral pattern (in particular, increased high-frequency activity) and improved performance in several domains. In visual cortex, for example, increased gamma power predicts faster reaction times in a perception task, perhaps related to increased neural synchrony and resultant facilitated information transfer (27). Intracranial investigations of human memory have shown that increased high-frequency activity and decreased-low frequency activity in temporal cortex predict improved verbal memory encoding (28,29), again perhaps reflecting the facilitatory effect of synchronized neuronal spiking (30). In PFC, we have previously shown that increased gamma power predicts improved performance on a cognitive interference task on a trial-by-trial basis (31), potentially reflecting optimal allocation of cognitive control resources relative to demand (32). These observations across brain regions mediating perception-to-action behaviors highlight the importance of gamma power as an indicator of neural coherence and a candidate biomarker of performance. While these previous studies and our own analyses relied on canonically defined frequency bands, there has been a recent push toward instead quantifying the aperiodic (1/f-like) component of neural activity (33,34). A decrease in low-frequency power and increase in high-frequency power may reflect an overall change in the slope of the spectrum. Future work could seek to quantify aperiodic shifts in neural signals and assess their relationship with depression severity.

In areas subserving cognitive processes, however, the relationship appears to be more complicated. Though insufficient application of cognitive resources leads to eroded performance in controlled decision-making tasks (31,32), unconstrained attentive resources can also be maladaptive. For example, constitutively high activity in PFC regions may be the physiological driver of the inappropriately sustained attention to the external environment (e.g., the ordering of objects in a desk drawer) or to internal feelings (e.g., certainty that the stove is off) characteristic of obsessive-compulsive disorder (35,36). The same requirement for balance is true in affective domains. For example, consider reward sensitivity, one of the cardinal features of positive affect (37). Whereas a hallmark feature of depression is insufficient reward sensitivity (38), inappropriately elevated reward-seeking behavior is pathognomonic of addiction disorders (38,39). Thus, in disorders such as depression, which include dysfunction in cognitive and affective domains (40), these competing forces must achieve balance to produce adaptive, euthymic behavior. More is not always better. Consequently, neurophysiological biomarkers of such states will likely be more complex.

We therefore extended our investigation beyond the observed correlations and built a decoder to predict depression severity from spectral power features. Due to the sparse sampling of symptom state relative to that of the electrophysiological data, we began with a model formulation forced to use only the smallest subset of regions, thus producing a model that is more generalizable and less prone to overfitting. The consistent selection of ACC in all patients speaks to the importance of this region in mood and cognitive regulation (26,41). Even as the region selectivity requirement was relaxed, the prominence of ACC remained (Figure 4). Although this brain region was commonly selected across patients, the predictive spectral features in ACC differed across participants. The features that were highly predictive were a subset of the features that showed significant correlations with depression severity. In patient 1, beta power was most predictive of depression severity, whereas in patients 2 and 3, high-gamma power was most predictive. This interindividual variability may reflect fundamental differences in how our brains encode complex phenomena such as cognition and emotion, possibly due to factors such as sex, gender, age, heterogeneity of depression subtypes, developmental history, or other genetic or environmental effects (42–46). Therefore, it is not surprising that some predictive features differ across participants. Interindividual variability in neural features important for decoding is common across various cognitive domains. Other studies have demonstrated considerable heterogeneity in predictive neural features across subjects for mood decoding (15), verbal memory (47,48), and speech decoding (49,50), as just a few examples. Continued efforts can test the hypothesis that certain features are common predictors across individuals, whereas other features are specific to the individual.

As seen in Figure 4, even though the ACC was the most predictive region for a reliable depression decoder in all patients, it was not the only one. Indeed, we found that features with significant predictive power were distributed across various prefrontal regions and frequency bands and were individual specific. This heterogeneity may reflect underlying differences in the involvement of depression-relevant regions across individuals. A growing body of work is attempting to associate differentially involved brain networks with the observed phenotypic diversity of depressive manifestations (45,46). Within this context, our results further underscore the complex nature of this disorder and the need to account for interindividual variability to optimally engage and treat symptomatic networks (45,46,51,52).

Previous studies have used both self-report questionnaires (14,15) and untethered task-free paradigms to study mood in patients with epilepsy (26). Due to the active self-evaluation of mood state required by questionnaires, decoders trained on data collected during ongoing assessments may be dependent on features related to the cognitive load of performing the task. In patient 3 in our study, we collected resting-state data immediately after CAT-DI administration and were able to use these neural data to predict depression severity with a comparable accuracy to that of the decoder trained on neural data collected during the CAT-DI assessment. The high similarity between the most predictive features across the two analyses argues that the features our model identified are indeed specific to depression severity. This similarity also suggests that these two ways of decoding mood (using recordings during an assessment vs. during a contiguous baseline period) may produce similar results, although further data are needed to test this emerging hypothesis.

Future efforts for decoding mood and affect will benefit from the development of continuous, objective behavioral markers (53). Currently, measuring these domains relies on administering behavioral assessments, a process that suffers from subjectivity and places a high burden on patients to frequently and accurately report their mental state. Contrast this situation with that of motor decoders, which enjoy the advantage of objective and highly temporally resolved measures of position, velocity, acceleration, and related variables (54–56). Promising methods for affective measures with comparable characteristics include using video and audio recordings (57). Incorporating facial expression and speech analysis may provide more extensive affective/emotional measures and thereby create the opportunity to develop better mood decoders.

ACKNOWLEDGMENTS AND DISCLOSURES

This work was supported by the National Institutes of Health (Grant No. UH3 NS103549 [to SAS, KRB, WKG, and NP], Grant No. K01 MH116364 [to KRB], Grant No. R21 NS104953 [to KRB], Grant No. UH3 NS100549 [to WKG and SAS], and Grant No. R01 MH114854 [to WKG]) and McNair Foundation (to SAS).

SAS and XP initiated the study. JX conceptualized analysis procedures, analyzed the data, and drafted the manuscript with support from NRP, JA, JM, RKM, PRS, ABP, AST, KRB, XP, and SAS. SAS, NP, WKG, SJM, and KRB oversaw the organization of the clinical trial, subject recruitment, and regulatory activities. JX, RKM, BM, JAA, ABA, VP, and DO performed data collection in the neurophysiology monitoring unit. RKM, BS, MER, and KRB performed magnetic resonance imaging analysis. XP, SAS, AST, ABP, PRS, and KRB supervised and guided the data analysis. JX, NRP, and SAS wrote the manuscript, and all authors contributed to review and revision of the manuscript.

We thank our study participants for their commitment and trust.

A previous version of this article was published as a preprint on medRxiv: https://doi.org/10.1101/2022.05.19.22275231.

SAS has consulting agreements with Boston Scientific, NeuroPace, Abbott, and Zimmer Biomet. WKG has received donated devices from Medtronic and has consulting agreements with Biohaven Pharmaceuticals. SJM is supported through the use of resources and facilities at the Michael E. DeBakey Department of Veterans Affairs Medical Center, Houston, Texas, and receives support from The Menninger Clinic. SJM has served as a consultant to Allergan, Alkermes, Axsome Therapeutics, BioXcel Therapeutics, Clexio Biosciences, Eleusis, EMA Wellness, Engrail Therapeutics, Greenwich Biosciences, Intra-Cellular Therapies, Janssen, Levo Therapeutics, Perception Neurosciences, Praxis Precision Medicines, Neumora, Neurocrine Biosciences, Relmada Therapeutics, Sage Therapeutics, Seelos Therapeutics, Signant Health, and Worldwide Clinical Trials. SJM has received research support from Biohaven Pharmaceuticals, Janssen, Merck, NeuroRx, Sage Therapeutics, and VistaGen Therapeutics. All other authors report no biomedical financial interests or potential conflicts of interests.

ARTICLE INFORMATION

From the Department of Neurosurgery, Baylor College of Medicine, Houston, Texas (JX, NRP, JM, RKM, BM, JAA, VP, DO, BS, MER, KRB, SAS); Department of Neuroscience, Baylor College of Medicine, Houston, Texas (JX, ABP, AST, XP); Department of Electrical and Computer Engineering, Rice University, Houston, Texas (JA, ABP, AST, XP); School of Engineering, Brown University, Providence, Rhode Island (ABA); Department of Psychiatry, Baylor College of Medicine, Houston, Texas (SJM, WKG); Department of Neurological Surgery, UT Southwestern Medical Center, Dallas, Texas (NP); Department of Computer Science and Engineering, University of Minnesota, Minneapolis, Minnesota (PRS); Department of Psychology, University of Minnesota, Minneapolis, Minnesota (PRS); and Center for Neuroscience and Artificial Intelligence, Baylor College of Medicine, Houston, Texas (ABP, AST, XP).

Address correspondence to Sameer A. Sheth, M.D., Ph.D., at sasheth@bcm.edu.

Received Aug 14, 2022; revised Jan 9, 2023; accepted Jan 25, 2023.

Supplementary material cited in this article is available online at https://doi.org/10.1016/j.biopsych.2023.01.020.

REFERENCES

1. Ferenczi EA, Zalocusky KA, Liston C, Grosenick L, Warden MR, Amatya D, *et al.* (2016): Prefrontal cortical regulation of brainwide circuit dynamics and reward-related behavior. Science 351:aac9698.
2. Hare BD, Duman RS (2020): Prefrontal cortex circuits in depression and anxiety: Contribution of discrete neuronal populations and target regions. Mol Psychiatry 25:2742–2758.
3. Carlén M (2017): What constitutes the prefrontal cortex? Science 358:478–482.
4. Allawala A, Bijanki KR, Goodman W, Cohn JF, Viswanathan A, Yoshor D, *et al.* (2021): A novel framework for network-targeted neuropsychiatric deep brain stimulation. Neurosurgery 89:E116–E121.
5. Hasin DS, Sarvet AL, Meyers JL, Saha TD, Ruan WJ, Stohl M, Grant BF (2018): Epidemiology of adult DSM-5 major depressive disorder and its specifiers in the United States. JAMA Psychiatry 75:336–346.
6. James SL, Abate D, Abate KH, Abay SM, Abbafati C, Abbasi N, *et al.* (2018): Global, regional, and national incidence, prevalence, and years lived with disability for 354 diseases and injuries for 195 countries and territories, 1990–2017: A systematic analysis for the Global Burden of Disease Study 2017. Lancet 392:1789–1858.
7. Greenberg PE, Fournier AA, Sisitsky T, Simes M, Berman R, Koenigsberg SH, Kessler RC (2021): The economic burden of adults with major depressive disorder in the United States (2010 and 2018). Pharmacoeconomics 39:653–665.

8. Köhler-Forsberg O, Cusin C, Nierenberg AA (2019): Evolving issues in the treatment of depression. JAMA 321:2401–2402.
9. Postorivo D, Tye SJ (2021): Novel antidepressant approaches for refractory depression. Curr Treat Options Psych 8:141–157.
10. Jelovac A, Kolshus E, McLoughlin DM (2013): Relapse following successful electroconvulsive therapy for major depression: A meta-analysis. Neuropsychopharmacology 38:2467–2474.
11. Carpenter LL, Janicak PG, Aaronson ST, Boyadjis T, Brock DG, Cook IA, *et al.* (2012): Transcranial magnetic stimulation (TMS) for major depression: A multisite, naturalistic, observational study of acute treatment outomes in clinical practice. Depress Anxiety 29:587–596.
12. Kellner CH, Knapp RG, Petrides G, Rummans TA, Husain MM, Rasmussen K, *et al.* (2006): Continuation electroconvulsive therapy vs pharmacotherapy for relapse prevention in major depression: A multisite study from the Consortium for Research in Electroconvulsive Therapy (CORE). Arch Gen Psychiatry 63:1337–1344.
13. González-Martínez J, Bulacio J, Thompson S, Gale J, Smithason S, Najm I, Bingaman W (2016): Technique, results, and complications related to robot-assisted stereoelectroencephalography. Neurosurgery 78:169–180.
14. Kirkby LA, Luongo FJ, Lee MB, Nahum M, Van Vleet TM, Rao VR, *et al.* (2018): An amygdala-hippocampus subnetwork that encodes variation in human mood. Cell 175:1688–1700.e14.
15. Sani OG, Yang Y, Lee MB, Dawes HE, Chang EF, Shanechi MM (2018): Mood variations decoded from multi-site intracranial human brain activity. Nat Biotechnol 36:954.
16. Gibbons RD, Weiss DJ, Pilkonis PA, Frank E, Moore T, Kim JB, Kupfer DJ (2012): Development of a computerized adaptive test for depression. Arch Gen Psychiatry 69:1104–1112.
17. Beiser D, Vu M, Gibbons R (2016): Test-retest reliability of a computerized adaptive depression screener. Psychiatr Serv 67:1039–1041.
18. Sheth SA, Bijanki KR, Metzger B, Allawala A, Pirtle V, Adkinson JA, *et al.* (2022): Deep brain stimulation for depression informed by intracranial recordings. Biol Psychiatry 92:246–251.
19. Fu Z, Beam D, Chung JM, Reed CM, Mamelak AN, Adolphs R, Rutishauser U (2022): The geometry of domain-general performance monitoring in the human medial frontal cortex. Science 376:eabm9922.
20. Hein G, Morishima Y, Leiberg S, Sul S, Fehr E (2016): The brain's functional network architecture reveals human motives. Science 351:1074–1078.
21. Sarafyazd M, Jazayeri M (2019): Hierarchical reasoning by neural circuits in the frontal cortex. Science 364:eaav8911.
22. Du L, Liu H, Du W, Chao F, Zhang L, Wang K, *et al.* (2018): Stimulated left DLPFC-nucleus accumbens functional connectivity predicts the anti-depression and anti-anxiety effects of rTMS for depression. Transl Psychiatry 7:3.
23. Scangos KW, Makhoul GS, Sugrue LP, Chang EF, Krystal AD (2021): State-dependent responses to intracranial brain stimulation in a patient with depression. Nat Med 27:229–231.
24. Banerjee A, Parente G, Teutsch J, Lewis C, Voigt FF, Helmchen F (2020): Value-guided remapping of sensory cortex by lateral orbitofrontal cortex. Nature 585:245–250.
25. Domenech P, Rheims S, Koechlin E (2020): Neural mechanisms resolving exploitation-exploration dilemmas in the medial prefrontal cortex. Science 369:eabb0184.
26. Bijanzadeh M, Khambhati AN, Desai M, Wallace DL, Shafi A, Dawes HE, *et al.* (2022): Decoding naturalistic affective behaviour from spectro-spatial features in multiday human iEEG. Nat Hum Behav 6:823–836.
27. Womelsdorf T, Fries P, Mitra PP, Desimone R (2006): Gamma-band synchronization in visual cortex predicts speed of change detection. Nature 439:733–736.
28. Burke JF, Long NM, Zaghloul KA, Sharan AD, Sperling MR, Kahana MJ (2014): Human intracranial high-frequency activity maps episodic memory formation in space and time. Neuroimage 85:834–843.
29. Greenberg JA, Burke JF, Haque R, Kahana MJ, Zaghloul KA (2015): Decreases in theta and increases in high frequency activity underlie associative memory encoding. Neuroimage 114:257–263.
30. Tong APS, Vaz AP, Wittig JH, Inati SK, Zaghloul KA (2021): Ripples reflect a spectrum of synchronous spiking activity in human anterior temporal lobe. Elife 10:e68401.
31. Haegens S, Pathak YJ, Smith EH, Mikell CB, Banks GP, Yates M, *et al.* (2022): Alpha and broadband high-frequency activity track task dynamics and predict performance in controlled decision-making. Psychophysiology 59:e13901.
32. Shenhav A, Botvinick MM, Cohen JD (2013): The expected value of control: An integrative theory of anterior cingulate cortex function. Neuron 79:217–240.
33. Pathania A, Euler MJ, Clark M, Cowan RL, Duff K, Lohse KR (2022): Resting EEG spectral slopes are associated with age-related differences in information processing speed. Biol Psychol 168:108261.
34. Donoghue T, Haller M, Peterson EJ, Varma P, Sebastian P, Gao R, *et al.* (2020): Parameterizing neural power spectra into periodic and aperiodic components. Nat Neurosci 23:1655–1665.
35. Milad MR, Rauch SL (2012): Obsessive-compulsive disorder: Beyond segregated cortico-striatal pathways. Trends Cogn Sci 16:43–51.
36. McGovern RA, Sheth SA (2017): Role of the dorsal anterior cingulate cortex in obsessive-compulsive disorder: Converging evidence from cognitive neuroscience and psychiatric neurosurgery. J Neurosurg 126:132–147.
37. Insel TR (2014): The NIMH Research Domain Criteria (RDoC) Project: Precision medicine for psychiatry. Am J Psychiatry 171:395–397.
38. American Psychiatric Association (2013): Diagnostic and Statistical Manual of Mental Disorders, 5th ed. Arlington, VA: American Psychiatric Association.
39. Volkow ND, Morales M (2015): The brain on drugs: From reward to addiction. Cell 162:712–725.
40. Otte C, Gold SM, Penninx BW, Pariante CM, Etkin A, Fava M, *et al.* (2016): Major depressive disorder. Nat Rev Dis Primers 2:16065.
41. Rolls ET (2019): The cingulate cortex and limbic systems for emotion, action, and memory. Brain Struct Funct 224:3001–3018.
42. Yao Z, Yan R, Wei M, Tang H, Qin J, Lu Q (2014): Gender differences in brain activity and the relationship between brain activity and differences in prevalence rates between male and female major depressive disorder patients: A resting-state fMRI study. Clin Neurophysiol 125:2232–2239.
43. Ancelin ML, Carrière I, Boulenger JP, Malafosse A, Stewart R, Cristol JP, *et al.* (2010): Gender and genotype modulation of the association between lipid levels and depressive symptomatology in community-dwelling elderly (the ESPRIT study). Biol Psychiatry 68:125–132.
44. Gururajan A, Clarke G, Dinan TG, Cryan JF (2016): Molecular biomarkers of depression. Neurosci Biobehav Rev 64:101–133.
45. Williams LM (2016): Precision psychiatry: A neural circuit taxonomy for depression and anxiety. Lancet Psychiatry 3:472–480.
46. Drysdale AT, Grosenick L, Downar J, Dunlop K, Mansouri F, Meng Y, *et al.* (2017): Resting-state connectivity biomarkers define neurophysiological subtypes of depression. Nat Med 23:28–38.
47. Ezzyat Y, Kragel JE, Burke JF, Levy DF, Lyalenko A, Wanda P, *et al.* (2017): Direct brain stimulation modulates encoding states and memory performance in humans. Curr Biol 27:1251–1258.
48. Ezzyat Y, Wanda PA, Levy DF, Kadel A, Aka A, Pedisich I, *et al.* (2018): Closed-loop stimulation of temporal cortex rescues functional networks and improves memory. Nat Commun 9:365.
49. Moses DA, Leonard MK, Makin JG, Chang EF (2019): Real-time decoding of question-and-answer speech dialogue using human cortical activity. Nat Commun 10:3096.

50. Cheung C, Hamiton LS, Johnson K, Chang EF (2016): The auditory representation of speech sounds in human motor cortex [published correction appears in Elife 2016;5:e17181]. Elife 5:e12577.
51. Du J, Rolls ET, Cheng W, Li Y, Gong W, Qiu J, Feng J (2020): Functional connectivity of the orbitofrontal cortex, anterior cingulate cortex, and inferior frontal gyrus in humans. Cortex 123:185–199.
52. Kupfer DJ, Frank E, Phillips ML (2012): Major depressive disorder: New clinical, neurobiological, and treatment perspectives. Lancet 379:1045–1055.
53. Provenza NR, Sheth SA, Dastin-van Rijn EM, Mathura RK, Ding Y, Vogt GS, *et al.* (2021): Long-term ecological assessment of intracranial electrophysiology synchronized to behavioral markers in obsessive-compulsive disorder. Nat Med 27:2154–2164.
54. Willett FR, Avansino DT, Hochberg LR, Henderson JM, Shenoy KV (2021): High-performance brain-to-text communication via handwriting. Nature 593:249–254.
55. Chaudhary U, Birbaumer N, Ramos-Murguialday A (2016): Brain–computer interfaces for communication and rehabilitation. Nat Rev Neurol 12:513–525.
56. Abbaspourazad H, Choudhury M, Wong YT, Pesaran B, Shanechi MM (2021): Multiscale low-dimensional motor cortical state dynamics predict naturalistic reach-and-grasp behavior. Nat Commun 12:607.
57. Dibeklioğlu H, Hammal Z, Cohn JF (2018): Dynamic multimodal measurement of depression severity using deep autoencoding. IEEE J Biomed Health Inform 22:525–536.